Quadrupole-Quadrupole Interactions to Control Plasmon-Induced Transparency

Goutam Rana,[1] Prathmesh Deshmukh,[2] Shalom Palkhivala,[2] Abhishek Gupta,[2] S. P. Duttagupta,[1] S. S. Prabhu,[2] VenuGopal Achanta,[2,*] and G. S. Agarwal[3]

[1]*Department of Electrical Engineering, Indian Institute of Technology, Bombay 400076, India*
[2]*Department of Condensed Matter Physics and Material Science, Tata Institute of Fundamental Research, Mumbai 400005, India*
[3]*Institute for Quantum Science and Engineering, Texas A&M University, TAMU4242, College Station, Texas 77843, USA*

(Received 12 December 2017; published 12 June 2018)

Radiative dipolar resonance with Lorentzian line-shape induces the otherwise dark quadrupolar resonances resulting in electromagnetically induced transparency (EIT). The two interfering excitation pathways of the dipole are earlier shown to result in a Fano line shape with a high figure of merit suitable for sensing. In metamaterials made of metal nanorods or antennas, the plasmonic EIT (PIT) efficiency depends on the overlap of the dark and bright mode spectra as well as the asymmetry resulting from the separation between the monomer (dipole) and dimer (quadrupole) that governs the coupling strength. Increasing asymmetry in these structures leads to the reduction of the figure of merit due to a broadening of the Fano resonance. We demonstrate a PIT system in which the simultaneous excitation of two dipoles result in double PIT. The corresponding two quadrupoles interact and control the quality factor (Q) of the PIT resonance. We show an antiresonancelike symmetric line shape with nonzero asymmetry factors. The PIT resonance vanishes due to quadrupole-quadrupole coupling. A Q factor of more than 100 at 0.977 THz is observed, which is limited by the experimental resolution of 6 GHz. From polarization-dependent studies we show that the broadening of the Lorentzian resonance is due to scattering-induced excitation of orthogonally oriented dipoles in the monomer and dimer bars in the terahertz regime. The high Q factors in the terahertz frequency region demonstrated here are interesting for sensing application.

DOI: 10.1103/PhysRevApplied.9.064015

I. INTRODUCTION

Scattering in subwavelength structures could mimic quantum mechanical phenomena in metamaterials [1]. The classical analogue of electromagnetically induced transparency (EIT) or plasmon-induced transparency (PIT) in metamaterials is one such phenomenon shown due to the coupling of a bright dipole mode in a monomer and the dark quadrupole mode in a dimer of a dolmen structure referred to as a plasmonic molecule [2]. PIT has since been demonstrated in a planar metamaterial made of a single and bilayered fish-scale pattern [3] for normal incidence excitation of split-ring-resonator molecules that are magnetoinductively or conductively coupled [4]. The Fano line shape and the PIT in plasmonic nanocavities are also shown in other structures like a coupled ring and disk system [5], a split ring sandwiched between two rods in which the simulated response from a single cell is compared with that from a periodic array [6], single dipole and dual-quadrupole coupling studies in a structure made of metal nanorods [6], among others [7–32]. Detailed studies of the dependence of Fano resonances on the parameters of the metamaterial-like period were reported in dolmen arrays [7,9]. In addition to the basic understanding of this interesting phenomenon, there are several proposed applications like slow light and sensing with a large figure of merit (FOM) [2,3,5,33]. The ways and means to control the Q factor and the FOM are of the utmost importance for eventual practical applications like sensing. Thus, it would be interesting to look at a possible way to control the PIT.

In a system where a discrete two-level system interacts with a continuum, the resultant Fano line shape is given by the expression [1],

$$\sigma = \frac{(\varepsilon + q)^2}{\varepsilon^2 + 1}, \tag{1}$$

where $\varepsilon = 2(E - E_0)/\Gamma$. E_0 is the resonance energy and Γ is the width of the discrete state and q is the shape or

*achanta@tifr.res.in

asymmetry parameter. When the asymmetry parameter is zero, a unique symmetrical dip appears for the Fano resonance. This is known as the antiresonance. It should be noted that, in Fano systems, large asymmetry results in a drop of the Q factor, and thus the FOM [1]. Thus, achieving a very high Q factor in the Fano systems is not easy.

EIT and PIT studies, so far, focused on understanding, manipulating, and applying the dipole-quadrupole interaction with the early studies on a three-level atomic system having interfering excitation pathways. Controlling the quadrupole mode could be interesting to get a handle on the dipole-quadrupole interaction and eventually the quality factor (Q) of the mode. To get a clearer understanding of the parameters that govern the Q factor, it would be helpful to study the effect of various factors on the observed Q factor of the PIT resonance. In addition, an optically excited second dipole, depending on the geometry, would induce another quadrupole with a relative phase different from the first quadrupole. Thus, the interference between the two quadrupoles could be used to control the Q factor of the PIT resonance and the spectral response, in general.

In this paper, we demonstrate such quadrupole-quadrupole coupling as a handle to control the Q factor of the PIT resonance. First, we present simulation and experimental results on a dolmen structure to elucidate the PIT mechanism in these structures followed by the role of a second dipole to induce a second quadrupole. We present detailed finite element method (FEM) simulations that are compared with experimental results in the terahertz frequency regime. A Q factor of more than 100 is demonstrated at 0.977 THz. In the symmetric system, we show the cancellation of the PIT due to the interference of two

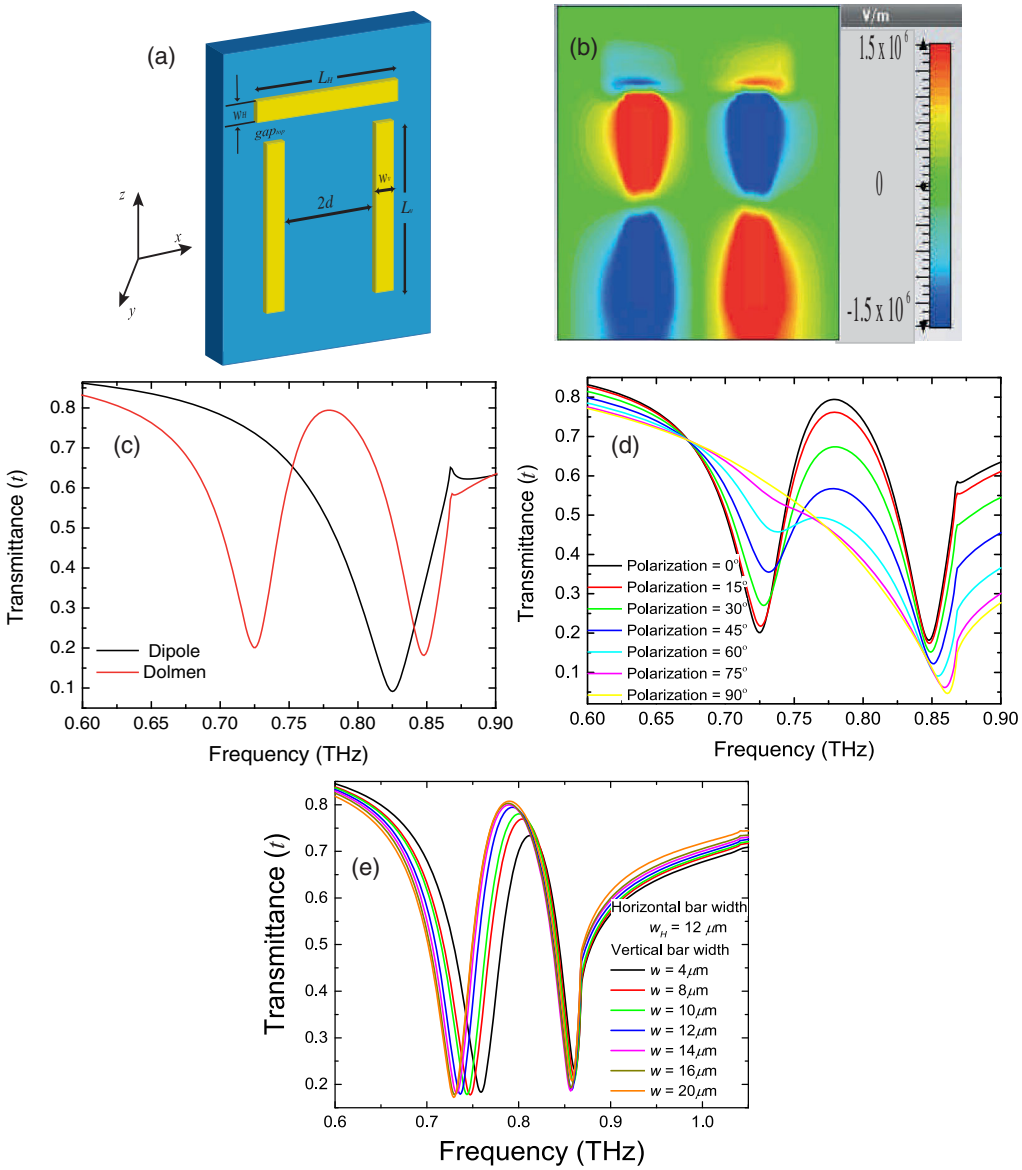

FIG. 1. (a) Schematic of the top view of the dolmen unit cell. (b) Electric field profile depicting the PIT condition in a dolmen with $d = 32$ μm and top gap $= 8$ μm for incident polarization such that the electric field is along the x direction. (c) Comparison of transmission spectra of dipole and dolmen structures. (d) Dependence of dolmen transmission spectrum on the polarization of the exciting terahertz wave. (e) Effect of width variation of the vertical bars of dolmen on the transmission spectrum.

quadrupole fields of exactly opposing phases similar to the antiresonance seen in a single Fano resonance with a zero asymmetry factor. We discuss various factors that affect the Q factor of the PIT resonances.

II. DESIGN CRITERIA

In the terahertz frequency range, one of the design criteria is to avoid the strong OH- absorption bands. Numerical studies are performed using FEM-based CST Microwave Studio® and the COMSOL Multiphysics® rf module. For gold, we use the Drude model with plasma frequency $\omega_p = 1.37 \times 10^{16}$ s^{-1} and damping frequency $\gamma = 0.009\omega_p$ [8]. For 150-nm-thick gold rods, the optimum dipole dimensions are length, 92 μm (L), and width, 12 μm (W) for the dipole resonance to be at 0.87 THz with a bandwidth of 0.39 THz. The dipole resonance strongly depends on the length of the monomer rather than its width or thickness (see Supplemental Material, Fig. S1 [34]). Three metal bars (monomers) are arranged in the dolmen shape with 64-μm ($2d$) separation between the two vertical bars forming the Dimer placed below the top monomer, as shown in the schematic of Fig. 1(a). With 8-μm space (gap_{top}) between the monomer and dimer, the otherwise dark quadrupole mode is excited by the dipole and the corresponding PIT peak arises at ~0.8 THz with approximately 0.073-THz bandwidth within the broad dipole resonance dip in transmission. The narrowest PIT peak is observed for a coupling distance of 12 μm (FWHM ~ 0.0216 THz) and the corresponding near-field profile is shown in Fig. 2(b). The influence of monomer-dimer separation (gap) and the distance between the dimer bars on the observed PIT is shown in the Supplemental Material, Figs. S2(a) and S2(b) [34], respectively. Figure 1(c) compares the transmission spectrum of a monomer and dolmen. The single dipole absorption in the monomer changes to a double dip in dolmen. To understand the origin of this, we perform polarization-dependent studies that clearly show [Fig. 1(d)] that the two dipole dip positions in the dolmen spectrum match with those corresponding to the two orthogonal incident polarizations that excite the dipoles in the horizontal and vertical monomers. In the visible-to-near IR region, the origin of the broadening is due to the metal dispersion [4]. However, in the terahertz region, where metals are perfect conductors, the broadening is due to scattering-induced excitation of dipoles in orthogonal monomers [Fig. 1(d)]. A maximal splitting is observed in the dolmen spectrum when identical metal bars form the monomer and dimer. A slight detuning of the two dipoles results in a narrower PIT resonance. An asymmetry in length introduces an asymmetry in the PIT peak, i.e., bonding and antibonding states differ due to different lengths of the coupled quadrupoles (Supplemental Material, Fig. S3 [34]). But an asymmetry in the monomer width affects the width of the PIT peak or the quadrupole bandwidth. The results are shown in the Supplemental Material, Fig. S1(b) [34]. Figure 1(e) shows the role of the width of the vertical bars (monomers) on the transmission spectrum. When the width of the vertical bars is increased, both the transmission dips narrow down. While the low-frequency state redshifts, the high-frequency state shows a very weak shift. These results indicate that the linewidth of

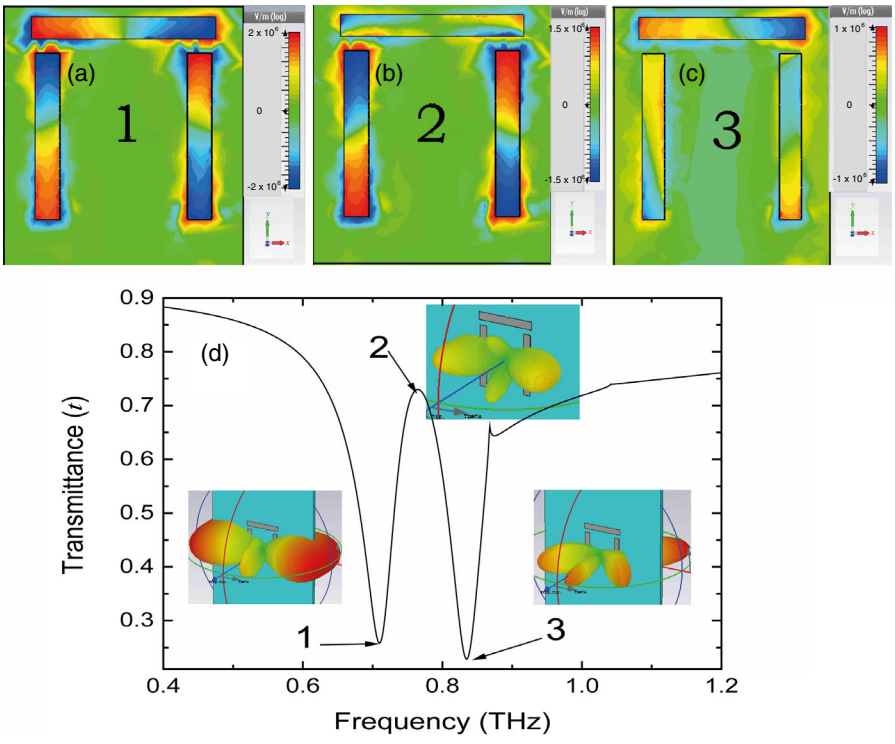

FIG. 2. Z component of the electric field (E_z) at different resonance frequencies [(a)–(c)] for the dolmen structure that are marked in the transmission spectrum (d).

the short-frequency Fano line shape is broader than that at higher frequency.

To enhance the signal-to-noise ratio in measurements, we study a 2D array of dolmen structures with a 120-μm period along the x axis, and a 144-μm period along the y axis. The dolmen array results in a PIT peak at 0.76 THz, which is redshifted from the single cell resonance. This well-known redshift is due to the coupling effects in an array of dolmens [9]. Near-field studies on dolmen arrays with randomly distributed array elements, which do not have the effect of periodicity, are also reported [35].

In a dolmen, the electric field profiles at three different frequencies of the transmission spectrum (transmission minima, and maximum labeled 1, 2, and 3 in Fig. 2, respectively) are studied to get an insight into the transparency mechanism [6,7]. At the PIT resonance frequency (marked 2 in Fig. 2), almost the entire energy of the bright dipole mode is coupled to the quadrupole mode in the vertical bars. It would be interesting to note that the field profiles [Figs. 2(a) and 2(c)] at the two transmission minima show out-of-phase quadrupole profiles in the vertical bars. The corresponding dipole in the horizontal bar remains the same (both amplitude and phase are similar).

So far, the focus of all the reported studies is on dipole-quadrupole coupling resulting in plasmon-mediated electromagnetically induced transmission (EIT) or absorption (EIA) or reflection mechanisms. We show above that by controlling the dipole-dipole interaction, the PIT peak width and, thus, the Q factor can be controlled to a lesser extent. However, the quadrupole-quadrupole coupling could be even more interesting to probe its utility as a handle to control the PIT peak width and thus the Q factor.

III. QUADRUPOLE-QUADRUPOLE INTERACTIONS

In a structure with a pair of inverted dolmens, the second dipole below the dolmen structure can be used as a handle to control the transmission spectrum. We show detailed simulation results below before the experimental demonstration.

The rectangular ringlike structure has one dolmen with a top gap of 8 μm and d of 32 μm, while the coupling strength has been varied by changing the bottom gap Fig. 3(b). The contour plot shows dispersion of the PIT molecular system where the hybridization of the PIT resonances can be seen. The transmission spectra show three dips and two peaks corresponding to the three dipoles and the two quadrupolar modes corresponding to PIT peaks. The dispersion plot shows that by varying the separation $(\mathrm{gap_{bottom}})$ and thus the coupling strength, the transmission spectrum as well as the quality factor of the PIT peaks can be controlled.

First, let us consider the interesting case of a symmetric structure which can be seen in Fig. 3(b) for $(\mathrm{gap_{bottom}})$ around 8 μm. When the structure is symmetric with both the monomers spaced equally away from the dimer $(\mathrm{gap_{top}} = \mathrm{gap_{bottom}})$, the near-field electric field distribution in Fig. 4(a) shows that the dipoles are in phase and there is no quadrupole mode in the dimer. Accordingly, we observe the complete disappearance of the PIT peak in the spectrum as shown in Fig. 4(b). The PIT peak vanishes as the equal but opposite phase quadrupoles induced by the top and bottom dipoles cancel each other. Though this is similar to the antiresonance expected in a Fano system when the asymmetry factor is set to zero, unlike in a single Fano resonance, the interaction between the two quadrupoles can be used to control the resonances in the ring structure.

In order to understand the role of the vertical bar width on the transmission resonances, we simulate the response for different widths. Results presented in Fig. 5, show that while the low-frequency resonance shifts considerably with the width of the vertical bar, there is little shift for the dipole resonance. Interestingly, the high-frequency resonance has very little shift in position, which will be discussed later. To elaborate the phase relation between the two dipoles and the induced quadrupoles, let us consider an asymmetric structure with the bottom gap reduced to 2 μm keeping the top gap as 8 μm. In Figs. 6(a)–6(e), we show the electric

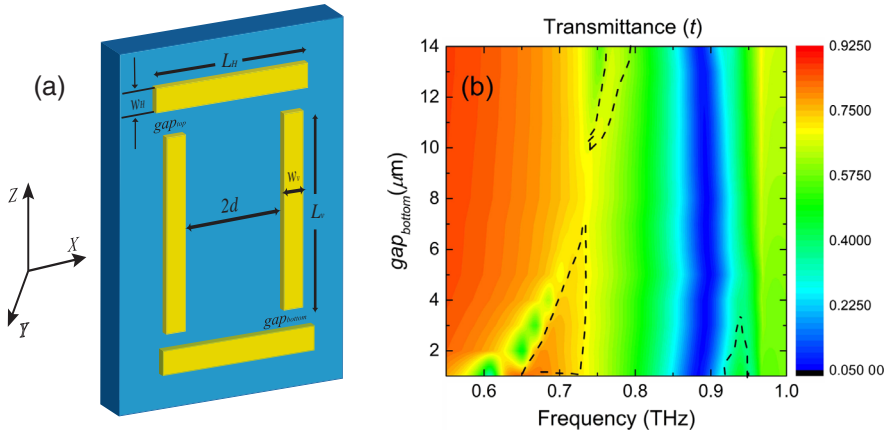

FIG. 3. (a) Top view of a unit cell of the rectangular ringlike structure, (b) 2D contour plot showing the dependence of transmission spectrum on the bottom gap. Regions inside the dashed contours (drawn to guide the eye) show the linewidth of the corresponding PIT peak.

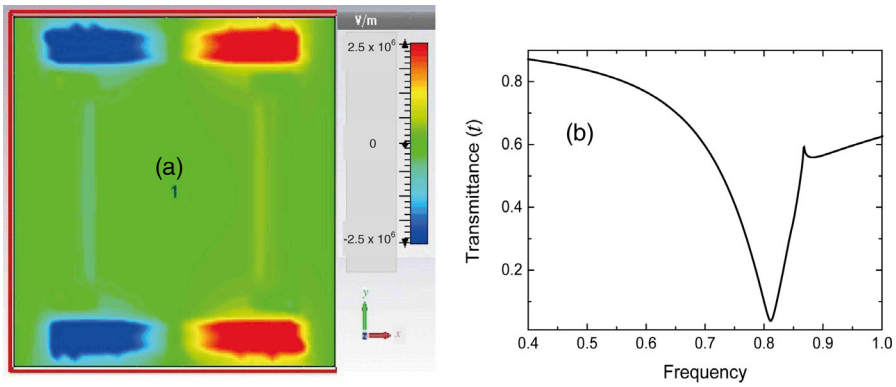

FIG. 4. Rectangular ringlike structure for equal coupling strength. (a) z component of electric field (E_z) for horizontal excitation and (b) transmission spectrum.

field profiles at the five different spectral positions that are labeled in the spectrum shown in Fig. 6(f). At spectral positions marked 1, 2, and 5, it is clear that the top dipole is modulated (and, thus, is different from the incident field) by the induced field in the dimer. Theoretically, it is shown that when the atomic density is high, due to cooperative effects, one would start seeing phase modulation. These are modeled by introducing incoherent excitations [36]. The scattering and dipole-induced modes contribute to similar phase modulation in the case of a pair of inverted dolmens and the calculated field profiles show these effects. Far-field profiles [insets in Fig. 6(f)] calculated show that each of the dips have a dipolar and the peaks have a quadrupolar profile. While the strong dipolar dip (labeled 3) has dipoles in both the bottom and top bars parallel to each other, the weaker dips labeled 1 and 5 correspond to antiparallel dipoles resulting in a net dipole absorption in the system. In the case of 3, the field profiles show that the dipoles induce a higher-order mode in each of the vertical bars. Because of the strong quadrupole excited by the bottom dipole, in the case of dips 1 and 5, there is an induced dipole in the top bar which is antiparallel to the dipole excited by the external field.

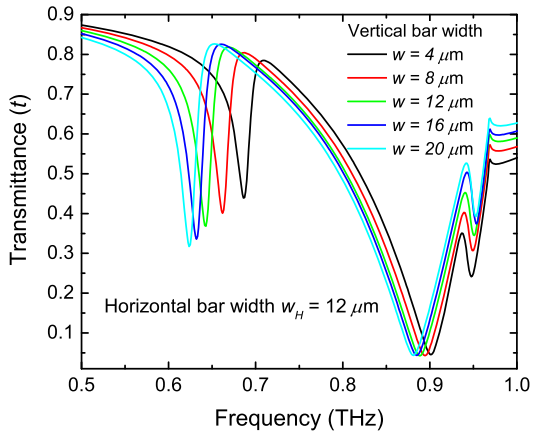

FIG. 5. Transmission spectra as a function of width of vertical bars with all other design parameters kept constant at length = 92 μm, top gap = 8 μm, bottom gap = 2 μm, d = 64 μm.

The strength of the dip or the net dipole in each case is a result of the external field-induced dipole and the quadrupole induced dipole. Out of the two quadrupolar peaks, labeled 2 and 4, field profile for 2 shows that the net dipole in the top bar is near negligible due to strong cancellation of the dipole due to incident field. So, the PIT is due to the bottom dipole-induced quadrupole. On the other hand, peak 4 corresponds to the higher-order mode induced by the net of bottom and top dipoles. However, from the near-field profiles shown in Fig. 6, the high-frequency dip and peak (labeled 3 and 4, respectively) are in fact a Fano

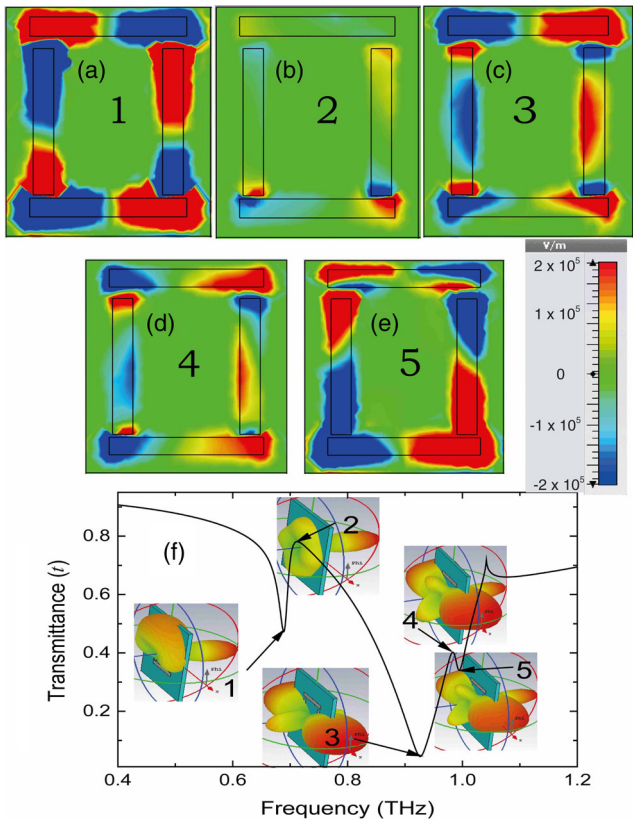

FIG. 6. (a)–(e) show the Z component of the electric field (E_z) at different frequencies labeled within the spectrum; (f) for an asymmetric structure with a top gap of 8 m and bottom gap of 2 μm.

resonance. A very small shift in their position with variation in the width of the vertical bars Fig. 5 as well as with the $\text{bottom}_{\text{gap}}$ [Fig. 3(b)] shows the behavior identical to the variation of the asymmetry factor (q) in Eq. (1). Further, the field profiles for 3 and 4 positions in the spectrum are nearly identical, showing that they possibly correspond to one Fano resonance. It would be interesting, nevertheless, to note that the far field of the dip (3) and peak (4) of the Fano line shape show dipole and quadrupole profiles, respectively.

It should be noted that the calculated far-field profiles for a single cell as well as the field distributions show that the observed multiple dips and peaks are due to the interaction of different modes excited in an inverted dolmen pair. Further, the strong dip labeled 3 in Fig. 6 matches with the dip in the symmetric case shown in Fig. 4(b). However, while in the asymmetric case there is still a net higher-order mode in the vertical monomers, in the symmetric case there is no net field. Overall, the transmission spectrum of a pair of inverted dolmens structure shows multiple Fano resonances.

IV. EXPERIMENTAL RESULTS

A dolmen and two inverted dolmen pair structures with 8- and 2-μm separation between the bottom dipole and the dimer are made by electron beam lithography followed by reactive ion etching of the gold with Ar plasma and residual resist removal by O_2 plasma. The gold patterns in 150-nm-thick gold are made on 500-μm fused silica substrates. Scanning electron microscope (SEM) images of the fabricated sample are shown in Fig. 7. Samples are studied using terahertz time-domain spectroscopy. Terahertz generated by a commercial BATOP antenna is transmitted through the structures and is measured using the electro-optic detection technique with a balanced photodetector pair. The frequency resolution of the measurement is 6 GHz. In order to avoid the artifacts arising from the back reflection of the terahertz pulse at the back surface of the substrate, a thick substrate is patched to the sample using index matching liquid from Cargille Laboratories (1809Y: RI series A, $n_0 = 1.536 \pm 0.0002$). Measurements are also tried by dipping the sample in the index matching fluid, but residual liquid removal from sample after measurements is an issue. A better alternative is to measure by sticking the sample on the window of a thick quartz cuvette filled with index matching liquid. This eliminates both the back-reflection problem as well as the sample surface contamination. As may be seen later from the experimental data of asymmetric ring structure, the reflected pulse can be completely suppressed.

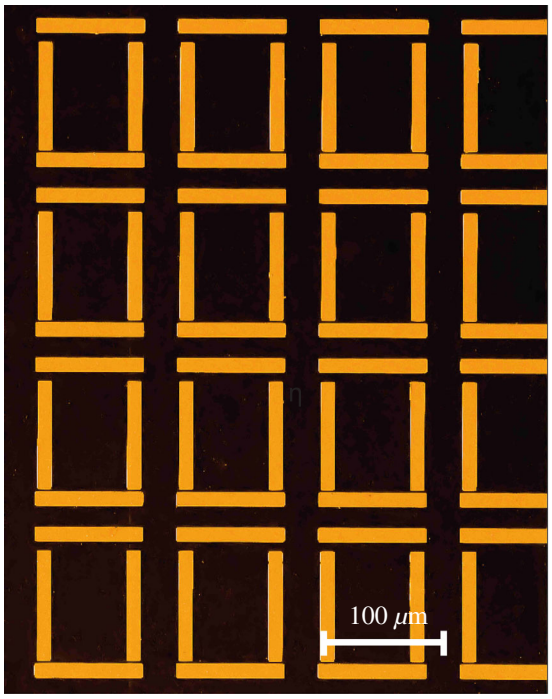

FIG. 7. SEM image of the fabricated rectangular ringlike structure.

Figure 8 shows the comparison of the measured (blue solid line) and simulated (green solid line) transmission spectra for a single dolmen [(a) and (b)] and the pair of inverted dolmens [(c),(d) for 8-μm bottom gap and (e),(f) for 2-m bottom gap]. While the dolmen structure shows the strong but broad PIT peak in both experiment and simulation [Figs. 8(a) and 8(b)], in the symmetric dolmen pair] with top and bottom gaps identical, Figs. 8(c) and 8(d)] the PIT peak vanishes due to the interference of out-of-phase quadrupoles induced by the top and bottom dipoles. On the other hand, for asymmetric structure due to unequal strengths of the induced quadrupoles, we observe two quadrupole field profiles at 0.81 and 0.966 THz [Figs. 8(e) and 8(f)]. It may be noted that the wriggles in the dolmen and symmetric ring data [Figs. 8(a) and 8(c)], are due to incomplete suppression of the reflected pulse from the back of the substrate. The asymmetric ring sample is optimized to suppress the back reflection. Figure S5 in the Supplemental Material [34] has the time-resolved data showing the back-reflected pulse.

In order to estimate the Q factors, the measured and simulated transmission spectra are fitted to multiple Fano lines. To get a consistent fit, the spectra calculated for different separations are fitted simultaneously. The main factors that govern the choice of widths (Γ) and asymmetric factors (q) are the positions of the dips and peaks, their relative heights, and the fact that the shift in the high-frequency dip is much weaker compared to the short-frequency dips as the coupling strength is varied. The latter observation implies that the width of the high-frequency mode is narrower than the short-frequency mode. The fits are presented with the

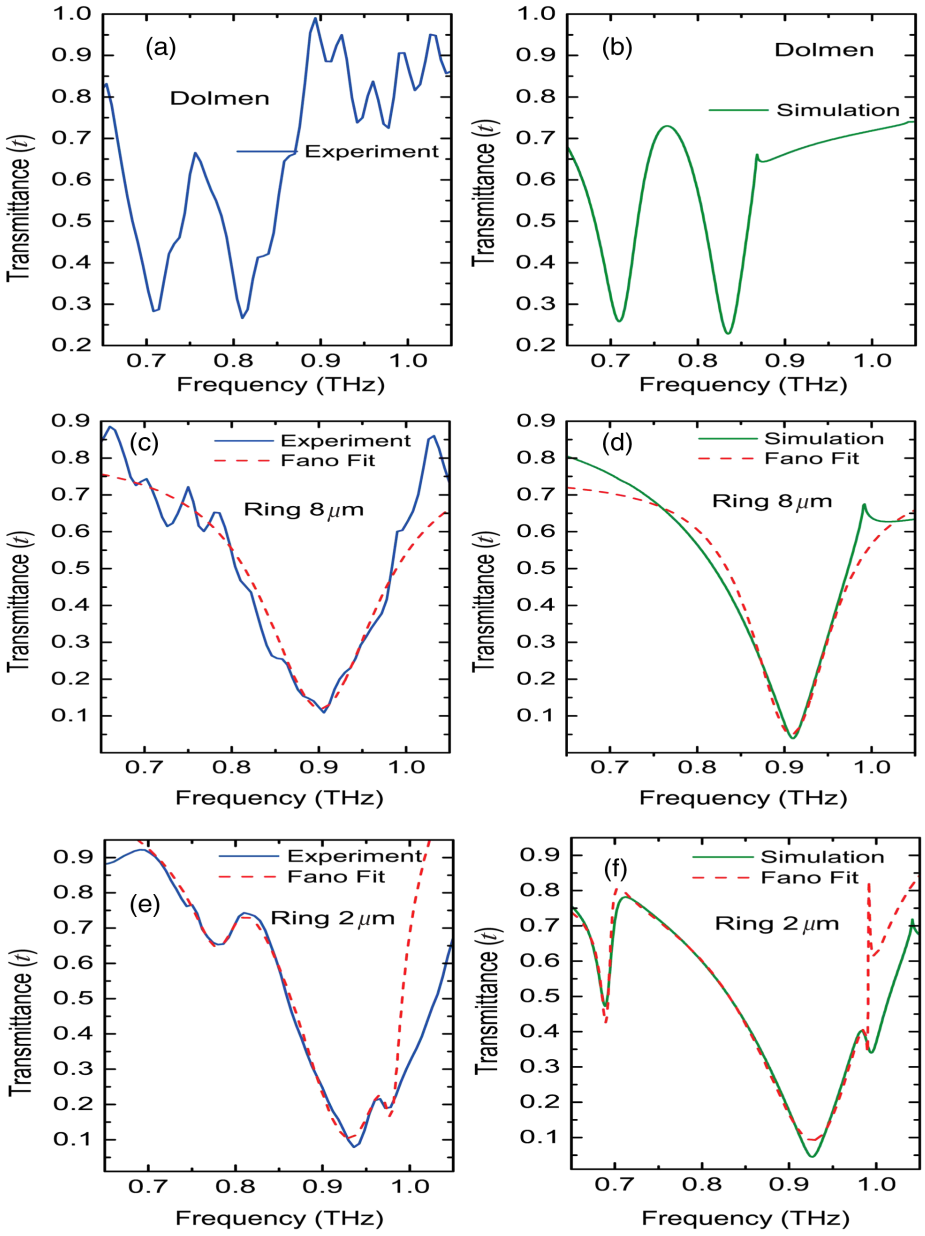

FIG. 8. Comparison of experimental (blue line) and simulation (green line) results on dolmen (a), (b) symmetric (c),(d), and asymmetric (e),(f) ringlike structures, respectively. Dashed red lines in (c)–(e) show the line-shape fit with three Fano resonances.

maximum possible widths that still retain the shift in dip position with varying coupling strength. In order to fit the residual component on the high-frequency side, a fourth resonance would be needed. Table I shows the fit parameters for the experimental and simulated spectra. The observed linewidths of the PIT peaks are much narrower compared to the dolmen structures with a quality factor as high as 100 at 0.977 THz extracted from the Fano line-shape fits. A three-level model that governs coupling of a single dipole and two quadrupoles is reported for the electromagnetically induced absorption case [37,38]. In the present work we have two

TABLE I. Fano line-shape fit parameters for the experimental and simulated transmission spectra for an asymmetric ring structure.

	E_0 (THz)		Γ (THz)		Q		Asymmetry factor (q)	
	Experiment	Simulation	Experiment	Simulation	Experiment	Simulation	Experiment	Simulation
1	0.788 ± 0.001	0.792 ± 0.001	0.06 ± 0.001	0.012 ± 0.001	13 ± 0.1	58 ± 0.1	0.45 ± 0.01	0.45 ± 0.01
2	0.949 ± 0.001	0.945 ± 0.001	0.151 ± 0.001	0.16 ± 0.001	6.3 ± 0.1	5.9 ± 0.1	0.23 ± 0.01	0.23 ± 0.01
3	0.977 ± 0.001	0.991 ± 0.001	0.01 ± 0.005	0.0015 ± 0.0003	100 ± 40	661 ± 40	0.5 ± 0.45	1.4 ± 0.3

dipoles and two quadrupoles which give one a handle to control the Q factor.

V. CONCLUSION

Electromagnetically induced transparency due to dipole-induced quadrupole resonance in plasmonic systems has interesting applications. As a sensor, its performance is limited by the Q factor and the figure of merit, and thus achieving a control on the Q factor is desirable. Our results show a narrowing of the PIT peak with the increasing width of the dimer bars in a dolmen. In dolmen at terahertz frequencies where the metal follows the Drude model, the broadening is due to scattered light which excites the orthogonal dipole in the vertical bars (that form the dimer). Further, we demonstrate quadrupole-quadrupole coupling as a means to control the PIT resonances and the Q factors. We experimentally demonstrate the expected broad PIT peak in the dolmen structure as well as narrow PIT peaks resulting from quadrupole-quadrupole interactions. A Q factor of about 100 is seen for the experimental peak at 0.977 THz. The results presented here show that a novel controllable response of PIT can be achieved in designed structures that make use of quadrupole-quadrupole interactions. In a symmetric structure, the PIT peak vanishes and a pure dipole dip is demonstrated due to the cancellation of quadrupolar fields. While the antiresonance of a Fano line shape arises when the asymmetry factor (q) is set to zero, a similar feature can be realized with $q \neq 0$ for each resonance in an inverted pair of dolmens where the quadrupole-quadrupole interactions cancel the PIT peak. This gives a better handle to control the Q factor.

[1] Andrey E. Miroshnichenko, Sergej Flach, and Yuri S. Kivshar, Fano resonances in nanoscale structures, Rev. Mod. Phys. **82**, 2257 (2010).

[2] Shuang Zhang, Dentcho A. Genov, Yuan Wang, Ming Liu, and Xiang Zhang, Plasmon-Induced Transparency in Metamaterials, Phys. Rev. Lett. **101**, 047401 (2008).

[3] N. Papasimakis, V. A. Fedotov, N. I. Zheludev, and S. L. Prosvirnin, Metamaterial Analog of Electromagnetically Induced Transparency, Phys. Rev. Lett. **101**, 253903 (2008).

[4] Na Liu, Stefan Kaiser, and Harald Giessen, Magnetoinductive and electroinductive coupling in plasmonic metamaterial molecules, Adv. Mater. **20**, 4521 (2008).

[5] Niels Verellen, Yannick Sonnefraud, Heidar Sobhani, Feng Hao, Victor V. Moshchalkov, Pol Van Dorpe, Peter Nordlander, and Stefan A. Maier, Fano resonances in individual coherent plasmonic nanocavities, Nano Lett. **9**, 1663 (2009).

[6] Jingjing Zhang, Sanshui Xiao, Claus Jeppesen, Anders Kristensen, and Niels Asger Mortensen, Electromagnetically induced transparency in metamaterials at near-infrared frequency, Opt. Express **18**, 17187 (2010).

[7] Masashi Miyata, Jumpei Hirohata, Yusuke Nagasaki, and Junichi Takahara, Multi-spectral plasmon induced transparency via in-plane dipole and dual-quadrupole coupling, Opt. Express **22**, 11399 (2014).

[8] Benjamin Gallinet and Olivier J. F. Martin, Influence of electromagnetic interactions on the line shape of plasmonic Fano resonances, ACS Nano **5**, 8999 (2011).

[9] Chen Yan and Olivier J. F. Martin, Periodicity-induced symmetry breaking in a Fano lattice: Hybridization and tight-binding regimes, ACS Nano **8**, 11860 (2014).

[10] Benjamin Gallinet and Olivier J. F. Martin, *Ab initio* theory of Fano resonances in plasmonic nanostructures and metamaterials, Phys. Rev. B **83**, 235427 (2011).

[11] Boris Luk'Yanchuk, Nikolay I. Zheludev, Stefan A. Maier, Naomi J. Halas, Peter Nordlander, Harald Giessen, and Chong Tow Chong, The Fano resonance in plasmonic nanostructures and metamaterials, Nat. Mater. **9**, 707 (2010).

[12] Dibakar Roy Chowdhury, John F. O'Hara, Antoinette J. Taylor, and Abul K. Azad, Orthogonally twisted planar concentric split ring resonators towards strong near field coupled terahertz metamaterials, Appl. Phys. Lett. **104**, 101105 (2014).

[13] T. J. Davis, D. E. Gmez, and K. C. Vernon, Simple model for the hybridization of surface plasmon resonances in metallic nanoparticles, Nano Lett. **10**, 2618 (2010).

[14] Toon Coenen, David T. Schoen, Sander A. Mann, Said R. K. Rodriguez, Benjamin J. M. Brenny, Albert Polman, and Mark L. Brongersma, Nanoscale spatial coherent control over the modal excitation of a coupled plasmonic resonator system, Nano Lett. **15**, 7666 (2015).

[15] Tingting Yin, Zhaogang Dong, Liyong Jiang, Lei Zhang, Hailong Hu, Cheng-Wei Qiu, Joel K. W. Yang, and Ze Xiang Shen, Anomalous shift behaviors in the photoluminescence of dolmen-like plasmonic nanostructures, ACS Photonics **3**, 979 (2016).

[16] Sushmita Biswas, Jinsong Duan, Dhriti Nepal, Ruth Pachter, and Richard Vaia, Plasmonic resonances in self-assembled reduced symmetry gold nanorod structures, Nano Lett. **13**, 2220 (2013).

[17] Sushmita Biswas, Jinsong Duan, Dhriti Nepal, Kyoungweon Park, Ruth Pachter, and Richard A. Vaia, Plasmon-induced transparency in the visible region via self-assembled gold nanorod heterodimers, Nano Lett. **13**, 6287 (2013).

[18] Odeta Limaj, Flavio Giorgianni, Alessandra Di Gaspare, Valeria Giliberti, Gianluca de Marzi, Pascale Roy, Michele Ortolani, Xiaoxing Xi, Daniel Cunnane, and Stefano Lupi, Superconductivity-induced transparency in terahertz metamaterials, ACS Photonics **1**, 570 (2014).

[19] Alp Artar, Ahmet A. Yanik, and Hatice Altug, Multispectral plasmon induced transparency in coupled meta-atoms, Nano Lett. **11**, 1685 (2011).

[20] Imogen M. Pryce, Koray Aydin, Yousif A. Kelaita, Ryan M. Briggs, and Harry A. Atwater, Highly strained compliant optical metamaterials with large frequency tunability, Nano Lett. **10**, 4222 (2010).

[21] Naresh K. Emani, Ting-Fung Chung, Alexander V. Kildishev, Vladimir M. Shalaev, Yong P. Chen, and Alexandra Boltasseva, Electrical modulation of Fano resonance in plasmonic nanostructures using graphene, Nano Lett. **14**, 78 (2014).

[22] Mario Hentschel, Thomas Weiss, Shahin Bagheri, and Harald Giessen, Babinet to the half: Coupling of solid and inverse plasmonic structures, Nano Lett. **13**, 4428 (2013).
[23] Yuanmu Yang, Wenyi Wang, Abdelaziz Boulesbaa, Ivan I. Kravchenko, Dayrl P. Briggs, Alexander Puretzky, David Geohegan, and Jason Valentine, Nonlinear Fano-resonant dielectric metasurfaces, Nano Lett. **15**, 7388 (2015).
[24] Xiaojun Liu, Jianqiang Gu, Ranjan Singh, Yingfang Ma, Jun Zhu, Zhen Tian, Mingxia He, Jiaguang Han, and Weili Zhang, Electromagnetically induced transparency in terahertz plasmonic metamaterials via dual excitation pathways of the dark mode, Appl. Phys. Lett. **100**, 131101 (2012).
[25] Ryohei Hokari, Yoshiaki Kanamori, and Kazuhiro Hane, Fabrication of planar metamaterials with sharp and strong electromagnetically induced transparency-like characteristics at wavelengths around 820 nm, J. Opt. Soc. Am. B **31**, 1000 (2014).
[26] Jianqiang Gu, Ranjan Singh, Xiaojun Liu, Xueqian Zhang, Yingfang Ma, Shuang Zhang, Stefan A Maier, Zhen Tian, Abul K Azad, Hou-Tong Chen, Antoinette J Taylor, Jiaguang Han, and Weili Zhang, Active control of electromagnetically induced transparency analogue in terahertz metamaterials, Nat. Commun. **3**, 1151 (2012).
[27] Yuanmu Yang, Ivan I. Kravchenko, Dayrl P. Briggs, and Jason Valentine, All-dielectric metasurface analogue of electromagnetically induced transparency, Nat. Commun. **5**, 5753 (2014).
[28] Jianjun Chen, Zhi Li, Song Yue, Jinghua Xiao, and Qihuang Gong, Plasmon-induced transparency in asymmetric *t*-shape single slit, Nano Lett. **12**, 2494 (2012).
[29] Hua Xu, Yuehui Lu, YoungPak Lee, and Byoung Seung Ham, Studies of electromagnetically induced transparency in metamaterials, Opt. Express **18**, 17736 (2010).
[30] Arif E. Çetin, Alp Artar, Mustafa Turkmen, Ahmet Ali Yanik, and Hatice Altug, Plasmon induced transparency in cascaded π-shaped metamaterials, Opt. Express **19**, 22607 (2011).
[31] Sher-Yi Chiam, Ranjan Singh, Carsten Rockstuhl, Falk Lederer, Weili Zhang, and Andrew A. Bettiol, Analogue of electromagnetically induced transparency in a terahertz metamaterial, Phys. Rev. B **80**, 153103 (2009).
[32] Yasuhiro Tamayama, Kanji Yasui, Toshihiro Nakanishi, and Masao Kitano, Electromagnetically induced transparency like transmission in a metamaterial composed of cut-wire pairs with indirect coupling, Phys. Rev. B **89**, 075120 (2014).
[33] Na Liu, Thomas Weiss, Martin Mesch, Lutz Langguth, Ulrike Eigenthaler, Michael Hirscher, Carsten Snnichsen, and Harald Giessen, Planar metamaterial analogue of electromagnetically induced transparency for plasmonic sensing, Nano Lett. **10**, 1103 (2010).
[34] See Supplemental Material at http://link.aps.org/supplemental/10.1103/PhysRevApplied.9.064015 for detailed analysis and clarification about simulation and characterization.
[35] Alexei Halpin, Christiaan Mennes, Arkabrata Bhattacharya, and Jaime Gmez Rivas, Visualizing near-field coupling in terahertz dolmens, Appl. Phys. Lett. **110**, 101105 (2017).
[36] Robert Fleischhaker, Tarak N. Dey, and Jörg Evers, Phase modulation induced by cooperative effects in electromagnetically induced transparency, Phys. Rev. A **82**, 013815 (2010).
[37] Kenan Qu and G. S. Agarwal, Phonon-mediated electromagnetically induced absorption in hybrid opto-electromechanical systems, Phys. Rev. A **87**, 031802 (2013).
[38] Xueqian Zhang, Ningning Xu, Kenan Qu, Zhen Tian, Ranjan Singh, Jiaguang Han, Girish S. Agarwal, and Weili Zhang, Electromagnetically induced absorption in a three-resonator metasurface system, Sci. Rep. **5**, 10737 (2015).